J. G. Foulkes, *ibid.*, p. 4715.
14. R. Derynck *et al.*, *EMBO J.* **7**, 3737 (1988).
15. S. B. Jakowlew, P. J. Dillard, P. Kondaiah, M. B. Sporn, A. B. Roberts, *Mol. Endocrinol.* **2**, 747 (1988).
16. S. B. Jakowlew, P. J. Dillard, M. B. Sporn, A. B. Roberts, *ibid.*, p. 1186.
17. P. Kondaiah *et al.*, *J. Biol. Chem.* **265**, 1089 (1990).
18. Y. Ogawa, D. K. Schmidt, J. R. Dasch, R.-J. Chang, C. B. Glaser, *ibid.* **267**, 2325 (1992).
19. Y. Ogawa, personal communication.
20. J. U. Bowie, R. Lüthy, D. Eisenberg, *Science* **253**, 164 (1991).
21. R. Lüthy, J. U. Bowie, D. Eisenberg, *Nature* **356**, 83 (1992).
22. S. Archer and D. Torchia, personal communication.
23. T. J. Richmond and F. M. Richards, *J. Mol. Biol.* **119**, 537 (1978).
24. C. Chothia, *Nature* **248**, 338 (1974).
25. M. Matsumura, W. J. Becktel, B. W. Matthews, *ibid.* **334**, 406 (1988).
26. A. E. Eriksson *et al.*, *Science* **255**, 178 (1992).
27. X.-F. Wang *et al.*, *Cell* **67**, 797 (1991).
28. F. Lopez-Casillas *et al.*, *ibid.*, p. 785.
29. S. Cheifetz and J. Massagué, *J. Biol. Chem.* **266**, 20767 (1991).
30. S. W. Qian *et al.*, *Proc. Natl. Acad. Sci. U.S.A.*, in press.
31. Purified mature TGF-β2, a recombinant form expressed in mammalian cells, was provided by Celtrix Pharmaceuticals, Inc. (Santa Clara, CA). The protein was supplied at 40 mg/ml in 0.1% trifluoroacetic acid, 40% acetonitrile, and was diluted four times with 10 mM acetate buffer pH 4.0. Crystals were grown from 10-μl drops consisting of equal parts of the diluted protein solution and well solvent. The well solvent contained 20% PEG 200, 50 mM sodium acetate buffer at pH 4.2 and 30 to 50 mM unbuffered sodium acetate added as precipitant. Typical crystals, measuring 0.5 mm by 0.5 mm by 0.3 mm, grew in about 10 days and diffracted to better than 2.0 Å. Crystals were stabilized with 10% PEG 200, 50 mM buffered sodium acetate at pH 4.2, and 50 mM unbuffered sodium acetate prior to data collection.
32. W. Kabsch, *J. Appl. Crystallogr.* **21**, 67 (1988).
33. _____, *ibid.*, p. 916.
34. The program package PHASIT was written and kindly provided by W. Furey.
35. W. A. Hendrickson and E. E. Lattman, *Acta Crystallogr.* **B26**, 136 (1970).
36. B.-C. Wang, *Methods Enzymol.* **115**, 90 (1985).
37. T. A. Jones, J.-Y. Zou, S. W. Cowan, *Acta Crystallogr.* **A47**, 110 (1991).
38. D. E. Tronrud, L. F. Ten Eyck, B. W. Matthews, *ibid.* **A34**, 489 (1987).
39. The sequence analysis program package GCG is the product of Genetics Computer Group, University of Wisconsin Biotechnology Center.
40. Y. Satow, G. H. Cohen, E. A. Padlan, D. R. Davies, *J. Mol. Biol.* **190**, 593 (1986).
41. T. N. Bhat, E. A. Padlan, D. R. Davies, Brookhaven Protein Data Bank entry 2FBJ.
42. C. K. Johnson, *ORTEP: A Fortran Thermal-Ellipsoid Plot Program For Crystal Structure Illustrations* (Oak Ridge National Laboratory, Oak Ridge, TN, 1970).
43. M. Carson, *J. Mol. Graphics* **5**, 103 (1987).
44. We thank D. Eisenberg for kindly providing the 3-D–1-D profile analysis programs and D. Torchia and M. B. Sporn for access to their unpublished results. Part of this work was done while K.A.P. was a Scholar-in-Residence at the Fogarty International Center, National Institutes of Health. The refined coordinates are being deposited in the Brookhaven Protein Data Bank.

22 May 1992; accepted 24 June 1992

Ocean Warming and Sea Level Rise Along the Southwest U.S. Coast

Dean Roemmich

Hydrographic time-series data recorded during the past 42 years in the upper 500 meters off the coast of southern California indicate that temperatures have increased by 0.8°C uniformly in the upper 100 meters and that temperatures have risen significantly to depths of about 300 meters. The effect of warming the surface layer of the ocean and thereby expanding the water column has been to raise sea level by 0.9 ± 0.2 millimeter per year. Tide gauge records along the coast are coherent with steric height and show upward trends in sea level that vary from about 1 to 3 millimeters per year.

Global sea level appears to be rising at a rate of about 2 mm/year (*1*, *2*). A variety of factors may contribute to sea level rise (*3*), including steric expansion of the water as a result of warming, an increase in the mass of water in the oceans as a result of glacial melting, and changes in the shape and volume of the ocean basins. A major step toward predicting future sea level rise and the impact of human activity on sea level is to distinguish the individual factors affecting the present sea level record. Moreover, if sea level rise is indicative of ocean warming, it is critical to determine the vertical distribution of the temperature change. The extent to which warming is concentrated in the surface layer must influence the ultimate impact of climate change on marine life. In this paper, I describe a study of long-term upper-ocean steric change with the use of a comprehensive regional hydrographic time series off California. The study focuses on the distribution of changes in steric height over position, depth, and time, and the relation of these changes to coastal sea level.

Repeated hydrographic and biological sampling along the California coast was initiated in 1950 and continues to the present. Stations in the sampling grid (Fig. 1) are typically 30 to 60 km apart, and the coverage at each station extends to depths of about 500 m in water up to 4 km deep. This survey, the California Cooperative Oceanic Fisheries Investigations (CalCOFI), has been carried out jointly by the state of California, the Scripps Institution of Oceanography, and the National Marine Fisheries Service. During the 1950s CalCOFI cruises were conducted up to ten times per year and coverage was extensive from Oregon to Baja California. The survey has been redefined several times. A serious hiatus in temporal resolution occurred during the 1970s, with only five cruises off southern California from 1969 to 1976. From 1984 to the present, sampling has been carried out quarterly along the six lines from San Diego to Point Conception (Fig. 1). I focus on this region.

CalCOFI Line 90 (Fig. 1) is the most heavily sampled of all the lines, with 170 repetitions. For each transect along Line 90, I interpolated the temperature and salinity data onto an evenly spaced grid with the use of an objective mapping procedure (*4*). I removed seasonal cycles independently at each grid point by subtracting the difference between the average over all cruises during a given month and the average over the 12 months. Nonseasonal residuals showed warming of nearly 1°C in the upper 100 m at all stations; at some stations warming was evident to depths of 300 m or more.

In order to help suppress sampling noise, data from each cruise were averaged horizontally over the highly sampled interval from station 90.35 (50 km offshore) to 90.70 (315 km offshore). For this interval, the vertically integrated effect of the temperature and salinity changes on the height of the sea surface is shown in a time series of steric height (*5*) (Fig. 1). Large positive offsets that occurred during the major El Niño episodes of 1957 to 1958 and 1982 to 1983 are notable in the steric height record. Steric height subsequently decreased after each episode but never fully returned to the pre–El Niño values. The trend in steric height from 1950 to the present shown in Fig. 1 amounts to 0.9 ± 0.2 mm/year. This trend is due to temperature change (Fig. 2B), with no substantial contribution from salinity. Line 93 off San Diego and Line 80 near Point Conception were also well sampled during the 42-year interval (138 and 132 transects); the results from these lines are similar to those from Line 90.

Net changes over the total length of the record are illustrated by averaging over the initial and final 7-year periods, from 1950 to 1956 and 1985 to mid-1991. These two intervals contained no major El Niño episodes. The steric height increase (Fig. 2A) was nearly 3 cm and, within the statistical uncertainty of the estimates, was spatially

Marine Life Research Group, Scripps Institution of Oceanography, La Jolla, CA 92093.

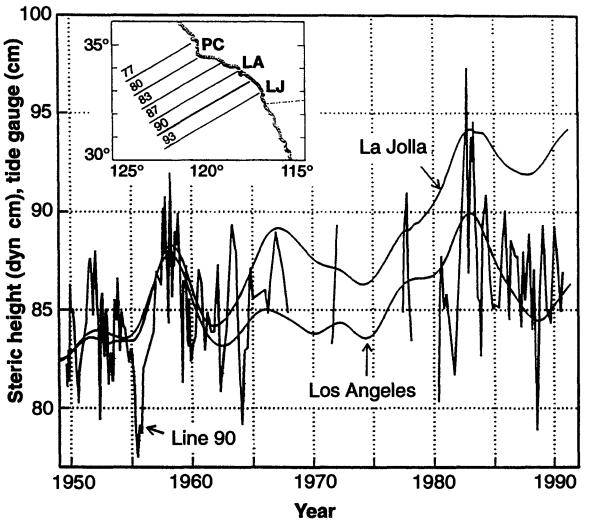

Fig. 1. Time series of steric height (0 relative to 500 dbar) for Line 90, the seasonal cycle removed, averaged between stations 90.35 and 90.70 (that is, from 50 to 310 km offshore). Smooth lines are low pass–filtered (using a Guassian with e-folding scale of 24 months) tide gauge data from Los Angeles and La Jolla, adjusted vertically to have the same height in 1950. The insert map shows locations of CalCOFI lines. PC, Point Conception; LA, Los Angeles; LJ, La Jolla. Units of steric height are given in dynamic centimeters (dyn cm). One dyn cm equals 10^3 dyne cm/g.

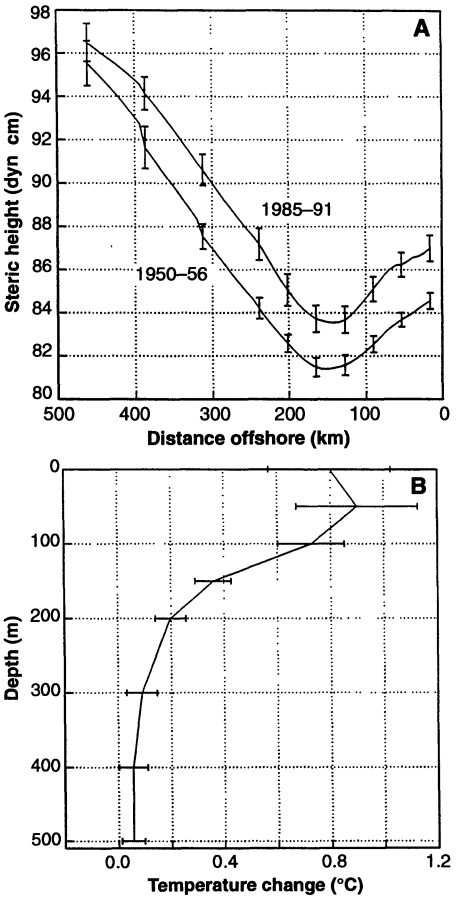

Fig. 2. (**A**) Steric height (0 relative to 500 dbar) as a function of distance offshore along line 90 for 1950 to 1956 (lower curve) and 1985 to mid-1991 (upper curve). Vertical bars indicate the standard error of the mean for each interval. (**B**) Temperature change as a function of depth between the intervals 1950 to 1956 and 1985 to mid-1991. Error bars indicate the sum of standard errors for the two intervals.

uniform. Again, results from lines 93 and 80 showed a similar increase. The slope of steric height with distance offshore indicates the structure of meridional geostrophic flow in the Southern California Bight; flow is northward near the shore and southward beyond about 150 km offshore. This is the familiar pattern of the California Current system in that the southward California Current lies offshore and a recirculation, the Southern California Eddy, is nearshore. The spatial uniformity in steric height increase (Fig. 2A) indicates that the large-scale warming and sea level rise were not accompanied by significant changes in the strength of the surface geostrophic circulation.

The temperature change between the initial and final 7-year periods (Fig. 2B) was about 0.8°C from the ocean surface to a depth of 100 m, 0.2°C at 200 m, and 0.1°C or less at 300 m and below. The CalCOFI dataset contains few stations much deeper than 500 m, and no conclusions can be drawn with regard to temperature fluctuations at greater depths. Time series of salinity do not show a significant trend at any depth.

Previous results (6) have suggested that the prevailing equatorward winds, which drive coastal upwelling and circulation along the California coast, have intensified substantially since 1950. Although one might anticipate cooler sea-surface temperatures near the coast and changes in the alongshore circulation as a result, neither of these effects was observed.

Comparison of the observed steric expansion with coastal tide gauge records presents a substantial problem. Although nearby coastal tide gauge records are highly coherent with steric height, they show different trends (Fig. 1). From 1950 to 1991, tide gauge records at Port San Luis, Santa Monica, Los Angeles, La Jolla, and San Diego—all within or near the boundaries of the CalCOFI survey—showed trends of 0.6, 0.6, 0.7, 2.5, and 2.3 mm/year, respectively. Douglas suggested (*1*) that the Los Angeles record be disregarded on the grounds of inadequate geodetic control as a result of subsidence caused by oil pumping. A model of the effect of postglacial rebound (*2*, *7*) indicates that, for sea level estimation, these records should be corrected by about 0.6 mm/year. Measurement of the vertical motion of tide gauge benchmarks is now feasible (*8*); but until this has been accomplished discrimination among the records is not justified. The observed range of trends in sea level within the CalCOFI region (1 to 3 mm/year) is also consistent with the estimated global sea level rise (*1*, *2*). I conclude that steric expansion of the upper 500 m off southern California accounts for between 30 and 100% of the sea level rise observed at adjacent coastal tide gauges.

The present findings cannot be extrapolated beyond the 42-year duration of this dataset or to other parts of the globe. The global pattern of steric variability may be very complex. A comparable rate of steric expansion was detected in a shorter (27-year) mid-ocean time series in the northeast Pacific (*9*); but there, 67% of the expansion occurred between 100 and 1000 m. In another 27-year time series, near Bermuda, steric height rose and fell on a decadal scale as a result of oscillations of the thermocline that were dominant over a steady warming at depths below 1500 m (*10*). Single repetitions of full water column hydrographic sections in the North Atlantic and South Pacific (*11*, *12*) have indicated both warming and cooling in alternating layers. Together, these studies suggest spatial and temporal complexity in global oceanic temperature changes; they also demonstrate the feasibility of using conventional hydrography to isolate steric changes from other physical effects in the sea level record.

Determination of the vertical distribution of warming is critical in order to anticipate the implications of a changing climate—it is not sufficient to simply determine the net steric expansion of the ocean. The finding of 0.8°C of warming in the upper 100 m of the ocean is of interest because of the concentration of plant and animal communities in the surface layer. The possible biological effects of temperature changes are not understood at the present time.

Ocean surface temperature records from the Scripps pier extend continuously from 1916 to the present. They show a similar warming trend between 1950 and 1991 to that seen in the offshore hydrography (0.024° ± .007°C per year for annual mean temperatures). There was no significant trend between 1916 and 1950, although the interval around 1950 was relatively cool.

The decade of the 1980s was the warmest on record, 0.4°C warmer on average than any other decade. Of the ten warmest years in the record, five have occurred since 1981. Although this temperature signal and the associated rise in steric height are not implausibly above the background level of decadal variability, the trend observed in the past 42 years is a matter for both strong concern and interest.

REFERENCES AND NOTES

1. B. C. Douglas, *J. Geophys. Res.* **96**, 6981 (1991).
2. W. R. Peltier and A. M. Tushingham, *Science* **244**, 806 (1989).
3. National Research Council Panel on Sea Level Change, *Sea Level Change*, R. Revelle, chairman (National Academy Press, Washington, DC, 1990).
4. F. P. Bretherton, R. E. Davis, C. B. Fandry, *Deep-Sea Res.* **23**, 559 (1976).
5. Steric height is the integral over pressure of specific volume anomaly, here from 500 dbar (equivalent to a depth of about 500 m) to the ocean surface. For example, the effect of warming the upper 100 dbar of the ocean, say from 15° to 16°C at a salinity of 34 practical salinity unit (psu), is to increase the thickness of that layer of water by 2.2 cm. In order to increase the thickness by the same fraction by salinity change, a decrease in salinity from 34 to about 33.7 psu would be required. The equation of state for seawater is given by: *Technical Papers in Marine Science 36* (Unesco, Paris, 1981).
6. A. Bakun, *Science* **247**, 198 (1990).
7. A. M. Tushingham and W. R. Peltier, *J. Geophys. Res.* **96**, 4497 (1991).
8. W. E. Carter *et al.*, *Woods Hole Oceanographic Institute Technical Report WHOI-89-31* (1989).
9. R. E. Thomson and S. Tabata, *Mar. Geod.* **11**, 103 (1987).
10. D. Roemmich, in *Sea Level Change*, National Research Council Panel on Sea Level Change, R. Revelle, chairman (National Academy Press, Washington, DC, 1990), chap. 13.
11. D. Roemmich and C. Wunsch, *Nature* **307**, 447 (1984).
12. N. Bindoff and J. Church, *ibid.* **357**, 59 (1992).

13. The many scientists and technical support personnel responsible for the existence and high quality of the CalCOFI data are gratefully acknowledged. This study was supported by the Scripps National Institution of Oceanography's Marine Life Research Group and by National Science Foundation grant 90-04230 (World Ocean Circulation Experiment).

9 March 1992; accepted 6 May 1992

Machining Oxide Thin Films with an Atomic Force Microscope: Pattern and Object Formation on the Nanometer Scale

Yun Kim and Charles M. Lieber*

An atomic force microscope (AFM) has been used to machine complex patterns and to form free structural objects in thin layers of MoO_3 grown on the surface of MoS_2. The AFM tip can pattern lines with ≤10-nanometer resolution and then image the resulting structure without perturbation by controlling the applied load. Distinct MoO_3 structures can also be defined by AFM machining, and furthermore these objects can be manipulated on the MoS_2 substrate surface with the AFM tip. These results suggest application to nanometer-scale diffraction gratings, high-resolution lithography masks, and possibly the assembly of nanostructures with novel properties.

The ability to manipulate matter and to assemble novel structures on the atomic to nanometer scale is currently a goal of many researchers in the physical and engineering sciences (*1–15*). One attractive strategy for achieving this goal is to use scanning probe microscopes, such as the scanning tunneling microscope (STM) or AFM, to move atoms or clusters of atoms directly into a desired configuration. For example, the STM has been used to remove single atoms from surfaces (*2, 3*), to position atoms on a surface (*4, 5*), and to create an atomic switch (*6*). On a nanometer scale the STM has also been used to create structures by field-assisted diffusion (*5, 7*), to develop organic resists (*8*), to expose passivated semiconductor surfaces (*9*), and to deposit gold islands on gold surfaces (*10*). Most recently the STM has been used to induce the dissociation of a single molecule on a silicon surface (*11*). In contrast, there are few examples of controlled, high-resolution manipulation with the AFM. Several groups have shown that direct contact (repulsive mode) imaging of soft organic layers under sufficiently high loads can lead to orientational ordering or removal or both of this organic layer from the area scanned by the AFM tip (*12, 13*). The length scale or resolution of these modifications typically has been ≥100 nm. In addition, AFM tip-induced wear of transition-metal dichalcogenide materials has been reported (*14, 15*) on a ≥50-nm scale. The results from these AFM studies are promising; however, the resolution and control of the surface features produced by the AFM are poor compared to structures created with the STM.

We believe that the materials used in these previous AFM studies have significantly limited the attainable resolution and selectivity. Hence, we have sought to explore the limits of direct surface manipulation with the AFM using a novel material system that consists of a thin (<50 Å) metal oxide film (MoO_3) on the surface of MoS_2. In comparison to previous studies, this system has several important features: (i) the thin MoO_3 film is rigid and nondeformable, in contrast to organic layers; (ii) MoO_3 can be selectively machined or imaged depending on the applied load of the AFM cantilever; and (iii) the MoS_2 substrate, which is a good lubricant, functions as an integral stop layer that automatically fixes the depth of the structures. We used this system to demonstrate controlled pattern development with ≤10-nm resolution and complex machining of movable objects that have nanometer dimensions. The generalization of these results to other materials and their potential applications to nanotechnologies are discussed.

Thin crystallites of α-MoO_3 were grown on the surface of single-crystal 2H-MoS_2 by thermal oxidation by using purified O_2 at 480°C for 5 to 10 min. The MoO_3 layers were identified by transmission electron diffraction, x-ray photoemission spectroscopy, and atomic-resolution AFM images (*16*). These studies have shown that α-MoO_3 (space group *Pbnm*) grows with the **b**-axis (13.848 Å) perpendicular to the MoS_2 substrate surface. For the above oxidation conditions, MoO_3 crystallites one to three unit cells thick (one unit cell = **b**-axis = 13.85 Å) and 200 to 500 nm on edge are formed. Additional details of the MoS_2 oxidation process and the characterization of the MoO_3 thin crystal layers will be discussed in detail elsewhere (*16*). All of the AFM experiments were carried out with a modified commercial instrument (Nanoscope, Digital Instruments, Santa Barbara, California). Si_3N_4 cantilever and tips (force constant $k \approx 0.38$ N/m) were used for imaging and modification. In addition, the AFM experiments were carried out in a nitrogen-filled glove box equipped with a purification system that reduced the concentrations of oxygen and water to less than 5 and 2 ppm, respectively. This environment enables us to obtain the reproducible conditions needed for controlled surface modification (*17*)

A typical image of a MoO_3 crystallite formed after thermal oxidation of MoS_2 at 480°C is shown in Fig. 1A. The MoO_3 has a thickness of ~15 Å (corresponding to one unit cell along **b**) and occupies most of the central portion of this 500 nm by 500 nm image. Atomic-resolution images confirm this structural assignment: the **a**-**c** plane of

Department of Chemistry and Division of Applied Sciences, Harvard University, Cambridge, MA 02138.

*To whom correspondence should be addressed.